Original Article

JCBFM

Journal of Cerebral Blood Flow & Metabolism
2019, Vol. 39(3) 513–523

DOI: 10.1177/0271678X17737012
journals.sagepub.com/home/jcbfm
SAGE

Tight coupling of astrocyte energy metabolism to synaptic activity revealed by genetically encoded FRET nanosensors in hippocampal tissue

Iván Ruminot[1,2], Jana Schmälzle[1], Belén Leyton[2,3], L Felipe Barros[2] and Joachim W Deitmer[1]

Abstract

The potassium ion, K^+, a neuronal signal that is released during excitatory synaptic activity, produces acute activation of glucose consumption in cultured astrocytes, a phenomenon mediated by the sodium bicarbonate cotransporter NBCe1 (*SLC4A4*). We have explored here the relevance of this mechanism in brain tissue by imaging the effect of neuronal activity on pH, glucose, pyruvate and lactate dynamics in hippocampal astrocytes using BCECF and FRET nanosensors. Electrical stimulation of Schaffer collaterals produced fast activation of glucose consumption in astrocytes with a parallel increase in intracellular pyruvate and biphasic changes in lactate. These responses were blocked by TTX and were absent in tissue slices prepared from NBCe1-KO mice. Direct depolarization of astrocytes with elevated extracellular K^+ or Ba^{2+} mimicked the metabolic effects of electrical stimulation. We conclude that the glycolytic pathway of astrocytes in situ is acutely sensitive to neuronal activity, and that extracellular K^+ and the NBCe1 cotransporter are involved in metabolic crosstalk between neurons and astrocytes. Glycolytic activation of astrocytes in response to neuronal K^+ helps to provide an adequate supply of lactate, a metabolite that is released by astrocytes and which acts as neuronal fuel and an intercellular signal.

Keywords

Organotypic hippocampal slices, FRET-nanosensors, neuronal activity, astrocyte metabolism, NBCe1

Received 6 April 2017; Revised 4 September 2017; Accepted 5 September 2017

Introduction

Neural activity is accompanied by fast changes in local extracellular glucose and lactate in the cerebral cortex.[1–5] These changes reflect the fast adaptation of local metabolism to the energy demands of neurons, mainly for the recovery of ion gradients challenged by excitatory synaptic activity and action potentials, a phenomenon termed neurometabolic coupling. While it is clear that most of the energy is consumed in neurons, astrocytes are interposed between blood-borne glucose and neurons, thus strategically poised to control the local consumption of glucose and production of lactate. The contribution of astrocytes to neurometabolic coupling has been investigated using diverse glucose analogues in culture, in tissue slices and in vivo, with conflicting results.[6–13] More direct measurement of glucose with a FRET-based nanosensor that permits the estimation of the glycolytic rate[14] has shown that extracellular K^+, which is released by neurons during excitatory synaptic activity and action potentials, induces fast glycolytic activation of astrocytes in culture, a phenomenon mediated by the sodium/bicarbonate cotransporter NBCe1.[15,16]

The present study was designed to investigate whether astrocytes also respond to K^+ in brain tissue, and whether the NBCe1 contributes to the glycolytic

[1]Abteilung für Allgemeine Zoologie, FB Biologie, University of Kaiserslautern, Germany
[2]Centro de Estudios Científicos (CECs), Valdivia, Chile
[3]Universidad Austral de Chile, Valdivia, Chile

Corresponding author:
Iván Ruminot, Centro de Estudios Científicos (CECs), Arturo Prat 514, Valdivia, Chile.
Email: iruminot@cecs.cl

response of astrocytes to excitatory neurotransmission. To this aims, we expressed the FRET glucose nanosensor in organotypical hippocampal slices prepared from NBCe1 KO mice, and also measured the dynamics of pyruvate and lactate in astrocytes. We opted for organotypical slices over acute slices as they are healthier from the metabolic point of view. The slicing procedure acutely depletes the slices of glycogen, which is followed by a recovery phase that varies among laboratories.[17–19] Organotypical slices have been shown to sustain gamma oscillations in the absence of glucose, in a DAB- and CP-316819-sensitive manner,[20] which indicates that two weeks in culture is an adequate period of recovery. Our results support a major role for extracellular K^+ and the NBCe1 in activity-dependent modulation of brain tissue glucose and lactate, and the astrocytic involvement in neurometabolic coupling.

Materials and methods

Standard reagents and inhibitors were acquired from Sigma. Adenoviral serotype four vectors encoding FRET sensors Ad FLII^{12}Pglu-700μΔ6,[21] Ad Pyronic[22] and Ad Laconic[23] were custom-made by Vector Biolabs. Fluo-4-AM and BCECF were purchased from Invitrogen.

Preparation of organotypic hippocampal slices

Procedures involving animals were carried out according to the Guide for the Care and Use of Laboratory Animals, National Research Council, USA. Procedures involving animals were approved by the Landesuntersuchungsamt Rheinland-Pfalz, Koblenz (23 177–07) and by the Centro de Estudios Científicos Animal Care and Use Committee. The reports of the procedures comply with the ARRIVE guidelines. Organotypic hippocampal slice (OHS) cultures were prepared as described by Stoppini et al.[24] and Schneider et al.[25] with some modifications. Briefly, hippocampal slices (400 μm) were cut with a McIlwain Tissue Chopper (Mickle Laboratory Engineering Company, United Kingdom) from five to seven-day-old C57BL/6 mice under sterile conditions. Slices were maintained on Biopore membranes (Millicell Standing Inserts, Merck Millipore, Germany) in an interface between a humidified normal atmosphere (5% CO_2, 36.5°C) and in a culture medium that consisted of 50% Minimal Essential Medium, 25% Hank's balanced salt solution, 25% horse serum plus 2 mM L-glutamine and 10 mM D-glucose at pH 7.4 in a Memmert incubator (Germany). The culture medium (1 ml) was replaced three times per week.

After seven days of culture, the slices were transduced by overnight incubation with 5×10^6 plaque-forming unit (PFU) of Ad FLII^{12}Pglu-700μΔ6, Ad Pyronic or Ad Laconic and imaged after another four to eight days.

NBCe1A KO mice were on a C57BL/6J background, with wild-type (WT) age-matched littermates serving as controls. Animals were genotyped by PCR analysis.[26]

Fluorescence imaging and Schaffer collateral stimulation

Detailed protocols describing the use of fluorescent glucose, pyruvate and lactate sensors are available.[21–23,27,28] Intact Biopore membranes carrying OHS were submerged into the recording chamber of a Zeiss LSM 700 confocal microscope or an upright microscope (BX50WI, Olympus) equipped with a monochromator (Polychrome IV, TILL Photonics), Optosplit (Cairn, UK) and a cooled CCD camera (TILL Photonics). The slices were continuously superfused at 2 ml/min with a 95%O_2/5% CO_2-gassed buffer containing (in mM): 136 NaCl, 3 KCl, 2 $CaCl_2$, 1 $MgCl_2$, 24 $NaHCO_3$, 1.25 NaH_2PO_4; 2 glucose, 1 lactate, pH 7.4 at room temperature (22–24°C). To estimate the rate of glucose consumption in single cells with a resolution of seconds, we used the glucose transporter blocker strategy.[14] For Ca^{2+} and H^+ imaging, OHS were loaded at room temperature for either 30 min with 5 μM Fluo-4 A-M or for 10 min with 2 μM BCECF A-M and imaged with a Zeiss LSM 700 confocal microscope while being continually superfused with a 95% O_2/5%CO_2-gassed buffer described above. Additionally, OHS were stained for 20 min with 0.5 μM sulforhodamine 101 to obtain astrocytic red fluorescent signals. Schaffer collaterals were stimulated using a Grass SD9 stimulator. Trains of electrical stimulation were applied to the hippocampal CA3 area with a frequency of 20 Hz and for a duration of 5 to 30 s at 10 V. Imaging was performed at a distance of 200 μm from the stimulation area.

Toluidine blue staining and immunohistochemistry

Slice cultures were fixed for 1 h in 4% paraformaldehyde and rinsed in PBS. Thereafter, slice cultures were exposed for 20 min to toluidine blue working solution, which was a mixture of 5 ml stock solution (1 g toluidine blue O in 100 ml of 70% ethanol) and 45 ml of 1% NaCl solution, pH 2.0–2.5. Thereafter, 96% ethanol (100 ml of 96% ethanol and four drops of acetic acid) was used for color differentiation of the staining. The differentiation step with strong acid removes nonspecific staining of weak acidic structures and, thus, increases the contrast between background and stained cells. The process was stopped with PBS after the

differentiation was clearly visible. After a brief rinsing with double-distilled water, slice cultures were placed on object plates and dried overnight. The slices were then exposed to xylol (Sigma-Aldrich) for 10 min and embedded with Entellan Neu (Merck Millipore).[25]

OHS expressing FRET-nanosensors were fixed for 1 h in 4% paraformaldehyde. The slices were then carefully washed three times in phosphate-buffered saline (PBS) for 5 min followed by incubation in citrate buffer (10 mM citric acid, 0.05% Tween 20, pH 6.0) for 20 min. Preincubation in blocking solution (3% bovine serum albumin, 10% normal goat serum, 0.1% Triton X-100) for 2 h was followed by incubation with the primary antibody (mouse anti-GFAP, BD Biosciences-US, 1:500) in PBS containing 3% bovine serum albumin overnight at 4°C. The following day, slices were washed three times in PBS for 5 min and then incubated for 2 h at room temperature with the secondary antibody (goat anti-mouse IgG coupled with Alexa 543) in PBS containing 5 μM Hoechst.

After a final washing step in PBS, slices were mounted on slides with self-hardening embedding medium (glycerol 40%, polyvinyl alcohol 16%, phenol 0.7%, Tris 0.05 mM). OHS were scanned with a Zeiss LSM 700 at a resolution of 2048 × 2048 pixels using the following sequential laser lines; 488 nm (Citrine), 534 nm (Alexa 543) and 440 nm (Hoechst).

Statistical analysis

Time courses illustrate the behaviour of representative single cells. Normality of distribution was tested using the Shapiro–Wilk test. Data are presented as means ± SEM. Differences in mean values were evaluated with the Student's *t*-test or with ANOVA. P values < 0.05 were considered statistically significant and are indicated with asterisk (*). P values > 0.05 were considered non-significant and are shown as N.S.

Results

Functional expression of FRET-based nanosensors in cultured OHS

In order to check the integrity and organization of the hippocampal tissue under culture conditions, we performed Toluidine blue staining at 7, 14 and 21 days in vitro (d.i.v.), with acute hippocampal slices used as a control. Figure 1(a) shows that the CA region and dentate gyrus can be easily distinguished at all d.i.v. We observed reduced cell density during culture as well as reduction of tissue thickness, attributable to cell death at the surface due to the slicing procedure and reorganization of the hippocampal tissue.[29] This occurs early within four to five days in vitro and is reaching a final thickness of between 150 and 200 μm.[24,30] Next, we tested the expression and sensitivity of the FRET nanosensors for glucose, pyruvate and lactate in OHS transduced with adenoviral vectors that have positive tropism to astrocytes. Glucose sensor expression was restricted to 30–40% of protoplasmic astrocytes along the hippocampal tissue, as confirmed by GFAP immunostaining in OHS expressing the glucose sensor (Figure 1(b)). The same pattern of expression was observed for the pyruvate and lactate nanosensors (Figure 1(d) and (e)). To estimate the dynamic range of the nanosensors for glucose, pyruvate and lactate in astrocytes from OHS, we saturated the glucose sensor with a saline solution containing 10 mM glucose (Figure 1(c)), the pyruvate nanosensor with a solution containing 3 mM pyruvate (Figure 1(d)) and the lactate nanosensor with a saline containing 10 mM lactate (Figure 1(e)), followed by removal of glucose, pyruvate and lactate, respectively. To deplete intracellular lactate and pyruvate, we take the advantage of a property of MCTs called transacceleration, which has been used in vitro to deplete intracellular lactate or pyruvate levels respectively in erythrocytes.[31] This effect is based on a property of monocarboxylate transporters (MCTs) called trans-acceleration, where the presence of extracellular monocarboxylates stimulates transporter substrate efflux. This process involves a facilitated conformational switch of the substrate binding site across the cell membrane when an adequate substrate is bound.[32–34] To deplete intracellular pyruvate and lactate, we trans-accelerated MCTs by adding 10 mM of lactate or monochloroacetate (MCA), respectively.

The astrocytic pyruvate signal does not significantly change upon lactate application (Figure 1(d)), indicating that the intracellular pyruvate concentration is virtually zero in the absence of glucose. The lactate signal is rapidly depleted upon the application of the non-metabolizable MCTs substrate monochloroacatate (Figure 1(e)), indicating that astrocytes maintain an intracellular pool of lactate, a phenomena also observed in astrocytes in vitro.[47] The delta ratio between saturation and deprivation of the glucose sensor was 26.9 ± 0.6% (Figure 1(c)), 35 ± 3.3% (Figure 1(d)) for the pyruvate nanosensor and 16.4 ± 1.2% (Figure 1(e)) for the lactate sensor. Similar responses were observed in FRET nanosensors expressed in primary astrocytic cultures.[14,22,23]

By using the in vitro K_D of the glucose sensor and the delta ratio obtained in Figure 1(c), we later estimated the basal glucose concentration in astrocytes from OHS. In the presence of 2 mM extracellular glucose, organotypic hippocampal astrocytes maintained a steady-state intracellular glucose concentration averaging 1.16 mM ($n = 23$ cells). This concentration is well over the K_M of hexokinase (50 μM) suggesting

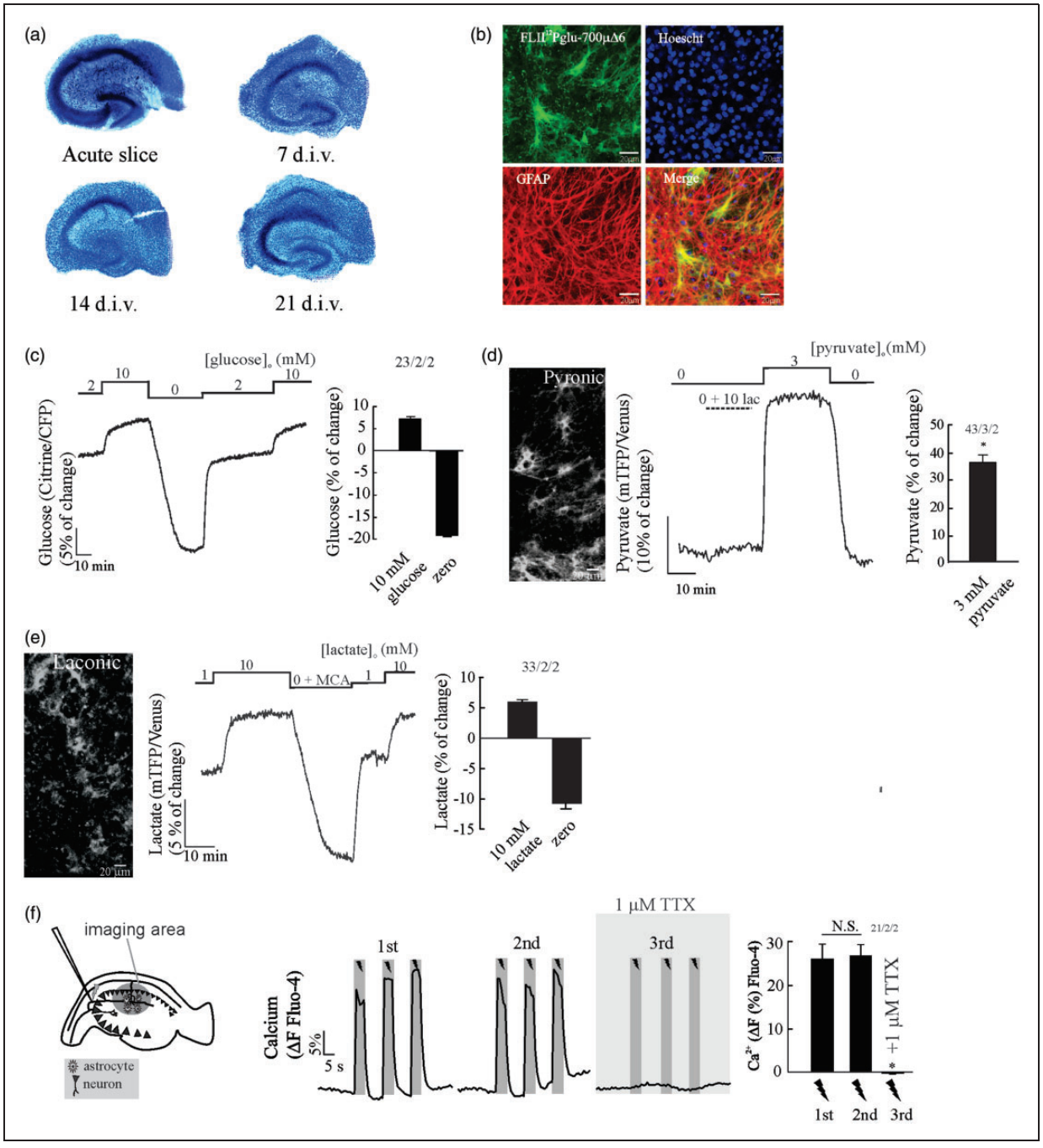

Figure 1. Dynamics of FRET-based nanosensors and integrity of cultured mouse organotypical hippocampal slices, OHS. (a) Toluidine blue staining shows that OHS morphology is preserved over a three-week cultivation period (d.i.v. = days in vitro) ($n = 3$, 2 animals). (b) Expression of the glucose sensor (FLIP^{12}Pglu-700 μΔ6) in OHS (bar is 20 μm). Confocal images show that the glucose sensor colocalises with the astrocytic marker GFAP, nuclei staining with Hoescht. (c) Dynamic range of the glucose nanosensor in astrocytes from OHS perfused with HCO_3^-/CO_2 saline. Cells were exposed to 2 mM glucose followed by the addition of 10 mM glucose and depleted by superfusion of saline without glucose. (d) Expression and dynamic range of the pyruvate sensor in astrocytes. Cells were exposed to a saline without extracellular pyruvate followed by application of 10 mM lactate and superfusion of 3 mM pyruvate. (e) Expression and dynamic range of the lactate sensor in astrocytes. Cells were exposed to a saline containing 1 mM lactate followed by application of 10 mM lactate and superfusion of 10 mM MCA to deplete intracellular lactate. All traces represent individual astrocytes. Bar graphs summarise the percentage of change after saturation or depletion of glucose, pyruvate and lactate nanosensors. (f) The Schaffer collateral stimulation in OHS loaded with Fluo-4 A.M in. The protocol consist of three trains of pulses (5 s at 20 Hz) separated by 3 min. The number of experiments is represented as n° of cells/ n°slices/ n°animals.

that glycolysis is not limited by glucose availability. Similar steady-state intracellular glucose concentration was obtained in a previous study using a similar protocol of organotypical slice preparation.[35] To evaluate the integrity and connectivity of the OHS, we performed Ca^{2+} imaging in CA1 by using electrical stimulus trains of 20 Hz for 5 s in CA3, a protocol that induces reliable extracellular K^+, Na^+ and Ca^{2+} transients in OHS.[36] Stimulation induced a robust and reproducible Ca^{2+} increase in cells located in the stratum radiatum of CA1 located 200 μm away from the stimulation electrode (Figure 1(f)). Ca^{2+} responses were suppressed in the presence of TTX (Figure 1(f)), indicating that (i) the electrical stimulation caused Ca^{2+} transients dependent on neuronal activity, and that (ii) the Ca^{2+} rise in CA1 is not caused by a stimulation artefact nor is it a result of direct depolarization by the electrode.

NBCe1 is required for K^+-dependent glycolytic activation in hippocampal astrocytes

Excitatory synaptic activity increases extracellular K^+, which depolarizes the highly K^+-permeable astrocytic plasma membrane. The astrocytic depolarization leads to the influx of bicarbonate via the abundant electrogenic sodium bicarbonate cotransporter NBCe1[37–41] resulting in cytosolic alkalinization and acute stimulation of glucose consumption.[16] To explore the relevance of this mechanism in hippocampal tissue, we have evaluated the effect of high extracellular K^+ (6 and 12 mM) on the rate of glucose consumption and intracellular pyruvate in astrocytes from OHS expressing glucose and pyruvate FRET-nanosensors. We observed a robust and dose-dependent activation of glucose consumption in WT hippocampal astrocytes upon increases of extracellular K^+, $252 \pm 3\%$ and $305 \pm 5\%$ of stimulation for 6 and 12 mM K^+, respectively (Figure 2(a) and (c)). We observed a significant reduction ($145 \pm 5\%$) in K^+-dependent glycolytic activation in hippocampal astrocytes from NBCe1-KO mice (Figure 2(a) and (c)). The K^+-dependent glycolytic activation was also present in OHS perfused with a cocktail of pre- (TTX) and postsynaptic inhibitors (MK-801 - CNQX), indicating that the stimulatory effect of K^+ is not mediated by neurons (Supp. Figure 1). To mimic membrane depolarization induced by extracellular K^+, we tested the effect of 3 mM Ba^{2+} on the rate of astrocytic glucose consumption. Barium elicited a glycolytic activation of similar magnitude to that induced by high K^+, but was dramatically diminished in hippocampal astrocytes from NBCe1-KO mice (Figure 2(b) and (c)). The concentration of Ba^{2+} used here has also been reported to block the Na/K-ATPase at the cytosolic side;[42] however, we did not observe inhibition of glycolysis, as shown previously for the known Na/K-ATPase blocker ouabain.[15] Considering that the effect of Ba^{2+} on astrocytic glycolysis was fully developed immediately after exposure, we think that a direct effect of Ba^{2+} on the Na/K-ATPase during the first seconds of exposure is probably minor.

Increased extracellular K^+ produced a sudden rise in intracellular pyruvate in WT astrocytes, but not in astrocytes from NBCe1-KO mice (Figure 2(d) and (e)). We conclude that the NBCe1 metabolic pathway is required for K^+- and Ba^{2+}-dependent glycolytic activation in hippocampal tissue. These signals depolarize astrocytes, stimulating NBCe1 in the inward going mode resulting in alkalinization and glycolytic activation in these cells.

Impact of neuronal activity on pH and glucose dynamics in astrocytes from WT and NBCe1-KO mice

Although an increased extracellular K^+ in the saline solution evokes a fast NBCe1-dependent activation of glucose consumption in astrocytes, there is no evidence that this glycolytic effect can be produced by endogenous K^+ released by neurons. To evaluate the impact of neuronal stimulation on astrocytic glucose, we applied three consecutive electrical stimulus trains of 20 Hz for 30 s, a protocol that induces reliable increases of extracellular K^+ in hippocampal slices.[36,43] As a control of NBCe1 activity, we performed H^+ imaging in astrocytes from OHS co-loaded with BCECF and sulforhodamine 101 (data not shown), a dye which is selectively taken up by astrocytes in the brain.[44] Upon stimulation, WT astrocytes responded with alkaline transients, in contrast to astrocytes from NBCe1-KO mice, which responded with small acid transients (Figure 3(b) to (d)). Furthermore, electrical stimulation evoked fast and reversible decreases of intracellular glucose concentration in WT astrocytes (Figure 3(e) and (g)), responses that were abolished by 1 μM TTX (Figure 3(f) and (g)). In contrast, hippocampal astrocytes from NBCe1-KO mice responded with a TTX-sensitive increase of intracellular glucose upon neuronal stimulation (Figure 3(h), (i) and (j)).

We conclude that neuronal stimulation leads to stimulation of NBCe1 with the consequent intracellular alkalinization and glycolytic activation in hippocampal astrocytes.[16,45,46]

Neuronal stimulation activates astrocytic glycolysis via the NBCe1 metabolic pathway

To explore the effect of neuronal activity on the rate of glycolysis, we estimated the rate of glucose consumption before and during neuronal stimulation in astrocytes from WT and NBCe1-KO mice.

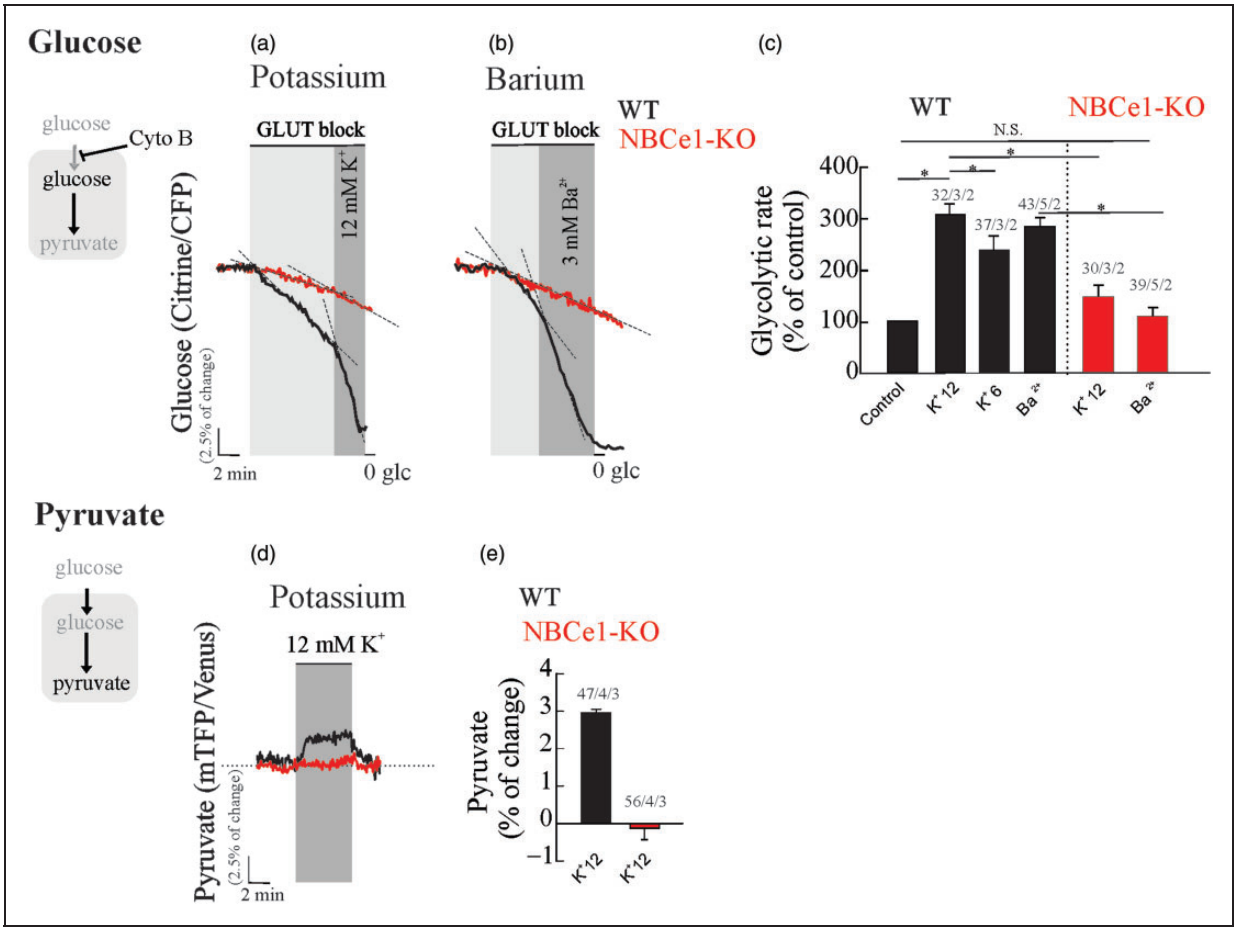

Figure 2. Astrocytic depolarization induced by K^+ or Ba^{2+} activates glycolysis in wild-type astrocytes but not in NBCe1-KO mice. Organotypical hippocampal astrocytes expressing the glucose sensor were continuously perfused with HCO_3^-/CO_2 buffer containing 2 mM glucose and 1 mM lactate. (a and b) Cytochalasin B (Cyto B, 20 μM) was applied to determine the effect of K^+ (6 and12 mM) or Ba^{2+} (3 mM) on the glucose consumption rate in WT and NBCe1-KO astrocytes. (c) Bar graphs summarise the percentage of glycolytic rate modulation upon stimulation with K^+ or Ba^{2+} in astrocytes from WT and NBCe1-KO mice. (d and e) Effect of K^+ (12 mM) on intracellular pyruvate from WT astrocytes and from NBCe1 KO mice. The number of experiments is represented as *n*° of cells/ *n*° slices/ *n*° animals.

Stimulation of Schaffer collaterals (20 Hz, 30 s) acutely activated astrocytic glycolysis in WT astrocytes (Figure 4(a) and (c)). Electrical stimulation did not alter the glucose consumption rate in hippocampal astrocytes from NBCe1-KO mice (Figure 4(b) and (c)). Taking advantage of a newly developed pyruvate FRET nanosensor,[22] we addressed the following question: Does acute glycolytic activation observed in astrocytes upon increased neural activity produce a rise in intracellular pyruvate, the end product of the glycolytic pathway? Astrocytes responded to neuronal activation with a rapid and reversible increase in intracellular pyruvate, a phenomenon that was absent in wild type slices perfused with 1 μM TTX and in astrocytes from NBCe1-KO mice (Figure 4(d) to (f)). To investigate whether the rise of pyruvate is instrumental to lactate increase upon glycolytic activation, we measured intracellular lactate[23] in wild type astrocytes challenged to neuronal activity. Upon neuronal stimulation, wild type astrocytes responded with an early fall in lactate, which was maintained or even recovered with an overshot during the stimulation protocol (Figure 4(g), (h) and (k)). The blocking of action potentials by TTX suppressed both lactate decrease and overshot (Figure 4(i) and (k)), indicating that both phenomena are dependent of neuronal signals released during the stimulation protocol. The early depletion of intracellular lactate, which also was reported recently in astrocytes in vitro and in vivo, has been attributed to the opening of a novel lactate-permeable chloride channel gated by cell depolarization.[47]

Discussion

We have used genetically encoded FRET-based nanosensors to explore the dynamics of energy metabolites

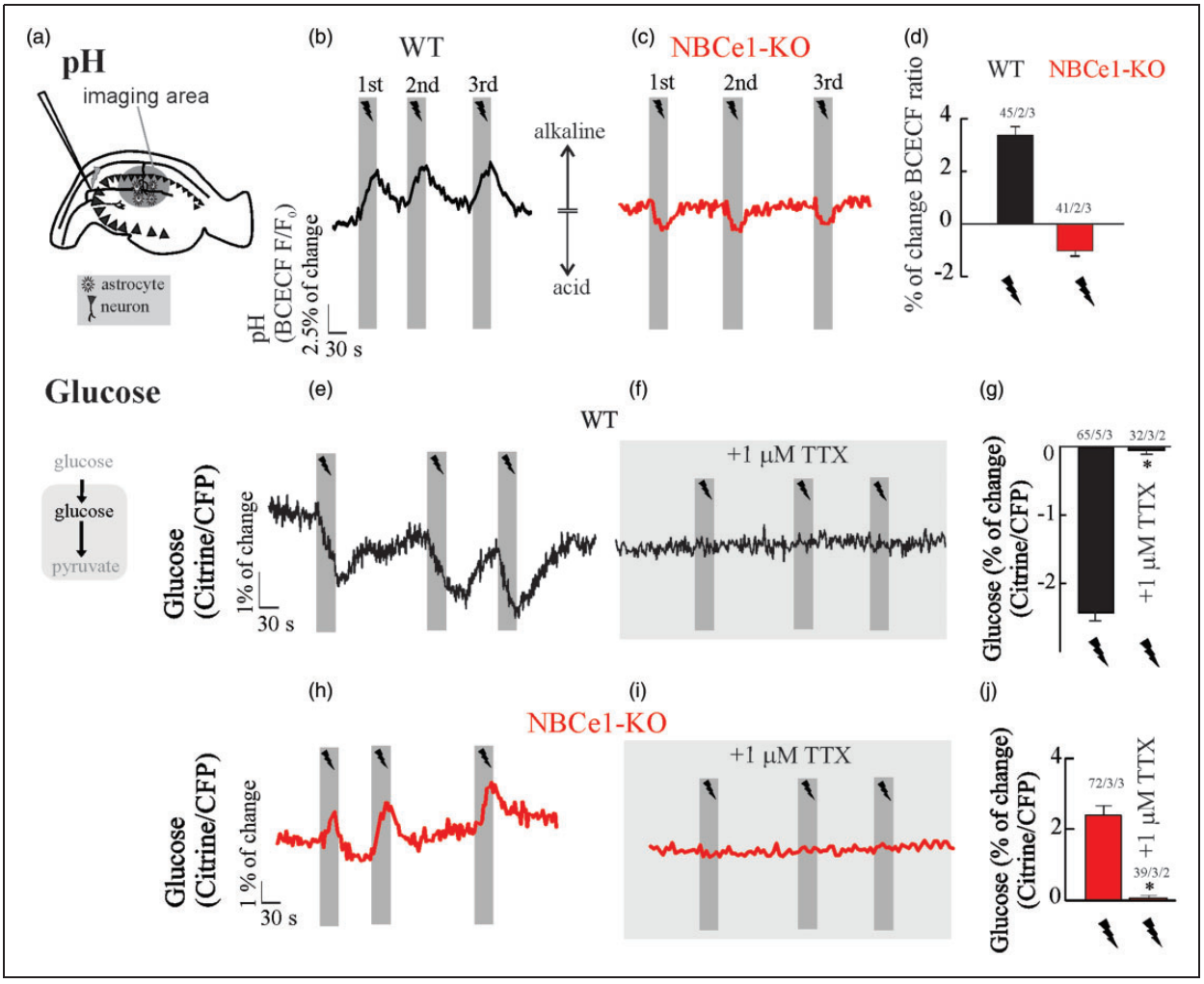

Figure 3. Neuronal activity causes alkaline transients and a drop in intracellular glucose in astrocytes from wild-type but not NBCe1-KO mice. (a–d) Effect of Schaffer collateral stimulation (20 Hz, 30 s) on intracellular pH in wild-type and NBCe1-KO organotypic hippocampal astrocytes loaded with BCECF-AM. (e–j) Effect of Schaffer collateral stimulation (20 Hz, 30 s) on intracellular glucose in wild-type and NBCe1-KO hippocampal astrocytes perfused with HCO_3^-/CO_2 saline containing 2 mM glucose and 1 mM lactate in the presence or absence of 1 μM TTX. All traces represent individual astrocytes. Bar graphs summarise the percentage of change of the BCECF-AM ratio or percentage of FRET change. The number of experiments is represented as *n*° of cells/ *n*° slices/ *n*° animals.

such as glucose, pyruvate and lactate in hippocampal astrocytes that surround active neurons. The two main findings of this work are: (i) astrocytic glycolysis is coupled to neuronal activity and (ii) the NBCe1 metabolic pathway plays a crucial role in neuron-glia metabolic coupling in hippocampal tissue. Excitatory synaptic activity induced by Schaeffer collateral stimulation caused a rapid activation of glucose consumption by hippocampal astrocytes and a concomitant rise in intracellular pyruvate. The glycolytic effect was effectively mimicked by increasing extracellular K^+ to an extent similar to that elicited by Schaeffer collateral stimulation.[36,37] Thus, we conclude that K^+ contributes a major part of the astrocytic glycolysis stimulation triggered by neuronal activity. As previously reported in cultured cells, the stimulation of glycolysis by K^+ in tissue slices was abrogated by genetic deletion of the NBCe1. The stimulation of astrocytic glycolysis has been attributed to pH rather than the simultaneous rise in intracellular bicarbonate.[45]

In spite of the activation of glucose consumption and accumulation of pyruvate, we observed a rapid decrease of intracellular lactate. Previously, a cytosolic reservoir of lactate was described in astrocytes in vitro and in vivo,[34,47] which is quickly released to the extracellular space by high extracellular K^+ and in response to electrical stimulation.[47] This phenomenon has been attributed to the opening of a novel 37 pS lactate-permeable chloride channel gated by cell depolarization, whose molecular identity is under current

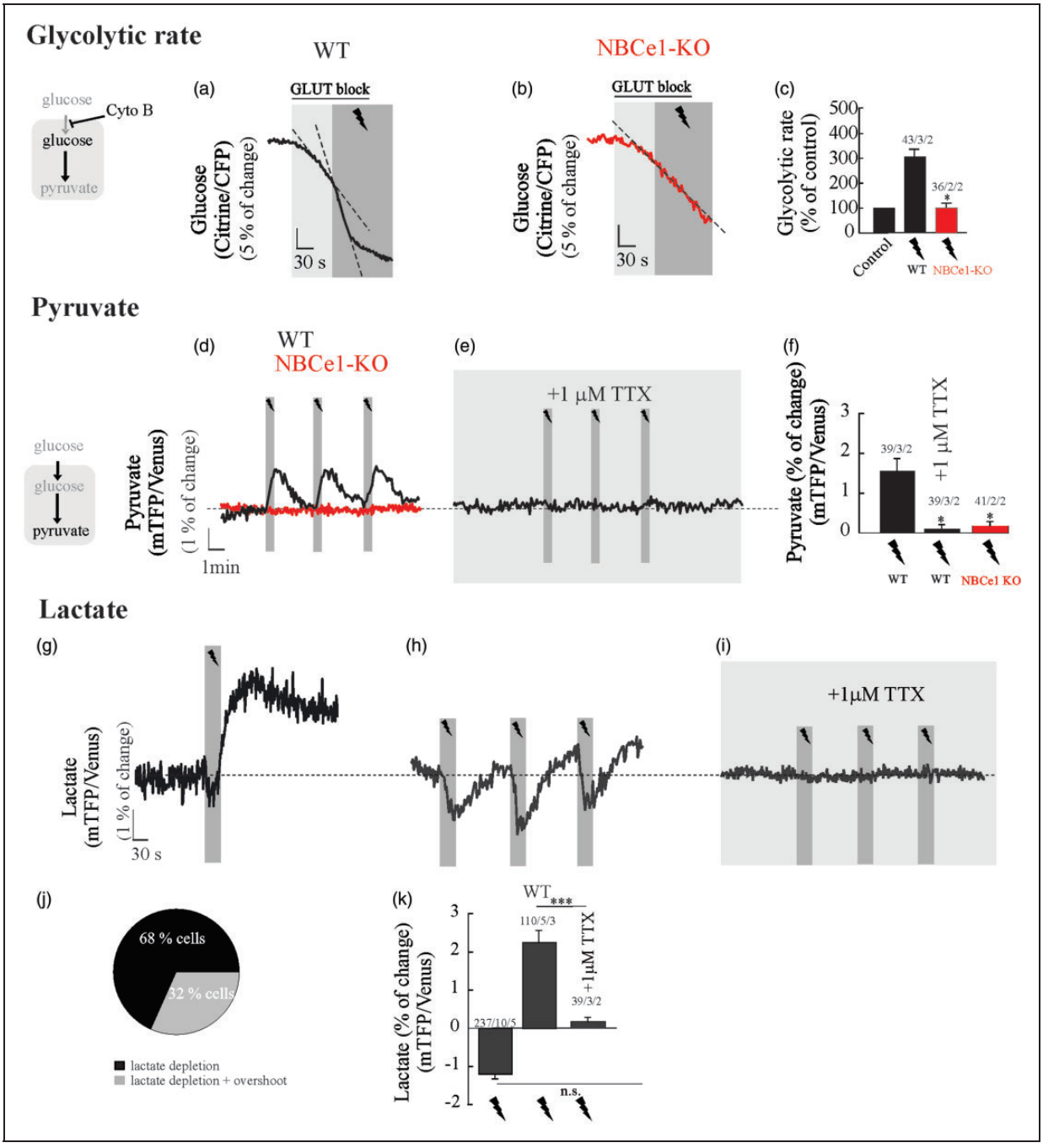

Figure 4. NBCe1 is required for fast glycolytic activation and a rise in pyruvate in hippocampal astrocytes challenged by neuronal stimulation. Glucose, pyruvate and lactate imaging in astrocytes from OHS perfused with HCO_3^-/CO_2 saline containing 2 mM glucose and 1 mM lactate. (a–c) Cytochalasin B (20 µM) was applied to block glucose transporters and determine the effect of neuronal stimulation on astrocytic glucose consumption in WT and NBCe1-KO astrocytes. (d–f) Effect of Schaffer collateral stimulation (20 Hz, 30 s) on intracellular pyruvate of astrocytes from WT and NBCe1-KO astrocytes perfused with HCO_3^-/CO_2 saline containing 2 mM glucose and 1 mM lactate in the presence or absence of 1 µM TTX in wild-type. (g–i, k) Effect of Schaffer collateral stimulation (20 Hz, 30 s) on intracellular lactate in astrocytes perfused with HCO_3^-/CO_2 saline containing 2 mM glucose and 1 mM lactate in the presence or absence of 1 µM TTX in wild-type. (j) Pie chart representing the distribution of lactate responses in WT astrocytes challenged to neuronal stimulation. All traces represent individual astrocytes. Bar graphs summarise the percentage of change of glucose, pyruvate or lactate FRET sensors upon stimulation/TTX in astrocytes from WT and NBCe1-KO hippocampal slices. The number of experiments is represented as n° of cells/ n° slices/ n° animals.

investigation. The sensitivity to TTX demonstrated for the first in the current study reinforces the notion that the astrocytic lactate depletion is mediated by a neuronal signal, i.e. K^+. Thanks to this channel astrocytes are capable of extruding lactate in spite the strong intracellular alkalinization induced by K^+,[47] a condition that is unfavorable for the housekeeping H^+-coupled MCTs. MCT-independent lactate extrusion from astrocytes has also been demonstrated for hemichannels[48] The increase in glucose consumption and pyruvate production mediated by K^+- NBCe1 may therefore be understood as a mechanism to replenish the astrocytic lactate reservoir.[34,47]

Report of activity-dependent rat astrocytic alkalinization in vivo[38,39] was followed by the demonstration in leech central nervous system[40] and rat hippocampus[41] that the pH change was mediated by stimulation of the NBCe1 by K^+-dependent membrane depolarization.[49] Recently, the kinetics of NBCe1-dependent alkalinization was found to closely follow astrocytic depolarization during evoked network activity in OHS.[50] RNAseq analysis and protein quantification have shown much stronger NBCe1 expression in astrocytes than in neurons, in both mouse and human.[51–53] We observed that afferent stimulation caused fast alkaline transients in WT astrocytes as compared with slight acidification transients in astrocytes from NBCe1-KO mice. The fact that in vivo cortical activity and evoked network activity in OHS resulted in astrocytic intracellular alkalinization shows that the effect of K^+ surpasses the acidification by glutamate.[16,54]

K^+ is released by active neurons during glutamatergic neurotransmission but also at Ranvier nodes during the action potential, at serotonergic synapses, and at cholinergic synapses, e.g. the neuromuscular junction. It therefore serves as a general signal for neurometabolic coupling. Glial cells are heterogeneous in terms of NBCe1 transporter, K^+ channel expression and resting membrane potential,[51,55] which may determine different basal NBCe1 activities, different pH responses to extracellular K^+ and perhaps different metabolic responses.

The role of extracellular K^+ acts as a modulator of glucose metabolism in astrocytes has been controversial. Some reports have shown that increased extracellular K^+ marginally activates[56–59] and even inhibits glucose metabolism in astrocytes.[60] With the benefit of hindsight, possible explanations for the diversity of results are exposure times, the presence of neurons in the cultures, and the presence of bicarbonate and supraphysiological K^+ in experimental solutions. Another metabolic effect of extracellular K^+ on astrocytes is the mobilization of glycogen mediated by the bicarbonate-sensitive soluble adenylate cyclase sAC.[61] The degradation of glycogen is also NBCe1-dependent but it seems to be much slower than the stimulation of glycolysis, because the rise in astrocytic cAMP levels occurred several minutes after the onset of K^+ stimulation.

The use of OHS cultures in combination with the expression of genetically-encoded FRET nanosensors for energy metabolites, provides optical access for imaging in single cells and allows the study of brain energy metabolism in tissue by using physiological concentrations of energy metabolites. Although many aspects of hippocampal slice cultures resemble the in vivo state,[62] excitatory neurons in this experimental system are known to exhibit increased axonal sprouting, which is likely to facilitate epileptiform activity.[63] Using organotypic slices also meant that the astrocyte population consisted of both protoplasmic astrocytes and reactive astrocytes, which is probably related to the trauma associated with the slicing procedure.[64] Worthy of special note is our observation of intracellular alkalinization and glycolytic activation in all astrocytic morphologies during neuronal stimulation, suggesting that metabolic coupling of astrocytes to neuronal activity is a general feature of astrocytes.

Based on the consistent results obtained in culture, in vivo and now in tissue slices, we propose that K^+ is the main signal responsible for fast neurometabolic coupling and that the astrocytic NBCe1 is the key element of its signal transduction pathway.

Funding

The author(s) disclosed receipt of the following financial support for the research, authorship, and/or publication of this article: This work was partly sponsored by the Deutsche Forschungsgemeinschaft [DE 231/25-1 to J.W.D.] and Fondecyt Grants [3160131 to I.R. and 1160317 to L.F.B.]. The Centro de Estudios Científicos (CECs) is funded by the Chilean Government through the Centers of Excellence Base Financing Program of CONICYT.

Acknowledgements

We thank M. Shefeeq Theparambil (London, U.K.) and Ignacio Fernández-Moncada (Valdivia, Chile) for helpful discussions, Oliver Kann, Andrea Lewen (Heidelberg, Germany) and Anne Thyssen (Kaiserslautern, Germany) for excellent technical assistance in the organotypic hippocampal slices preparation, Gary E. Shull (Cincinnatti, U.S.A.), for providing NBCe1-KO mice and Karen Everett and Amber Philp (Valdivia, Chile) for critical reading of the manuscript.

Declaration of conflicting interests

The author(s) declared no potential conflicts of interest with respect to the research, authorship, and/or publication of this article.

Authors' contributions

IR and JWD conceived the project and designed experiments. IR, JS and BL performed experiments and analyzed the data.

LFB developed a method and contributed to research material. IR wrote the paper.

Supplementary material

Supplementary material for this paper can be found at the journal website: http://journals.sagepub.com/home/jcb

References

1. Prichard J, Rothman D, Novotny E, et al. Lactate rise detected by 1H NMR in human visual cortex during physiologic stimulation. *Proc Natl Acad Sci U S A* 1991; 88: 5829–5831.
2. Hu Y and Wilson GS. A temporary local energy pool coupled to neuronal activity: fluctuations of extracellular lactate levels in rat brain monitored with rapid-response enzyme-based sensor. *J Neurochem* 1997; 69: 1484–1490.
3. Hu Y and Wilson GS. Rapid changes in local extracellular rat brain glucose observed with an in vivo glucose sensor. *J Neurochem* 1997; 68: 1745–1752.
4. Newman LA, Korol DL and Gold PE. Lactate produced by glycogenolysis in astrocytes regulates memory processing. *PloS One* 2011; 6: e28427.
5. Li B and Freeman RD. Neurometabolic coupling between neural activity, glucose, and lactate in activated visual cortex. *J Neurochem* 2015; 135: 742–754.
6. Pellerin L and Magistretti PJ. Glutamate uptake into astrocytes stimulates aerobic glycolysis: a mechanism coupling neuronal activity to glucose utilization. *Proc Natl Acad Sci U S A* 1994; 91: 10625–10629.
7. Loaiza A, Porras OH and Barros LF. Glutamate triggers rapid glucose transport stimulation in astrocytes as evidenced by real-time confocal microscopy. *J Neurosci* 2003; 23: 7337–7342.
8. Barros LF, Courjaret R, Jakoby P, et al. Preferential transport and metabolism of glucose in Bergmann glia over Purkinje cells: a multiphoton study of cerebellar slices. *Glia* 2009; 57: 962–970.
9. Chuquet J, Quilichini P, Nimchinsky EA, et al. Predominant enhancement of glucose uptake in astrocytes versus neurons during activation of the somatosensory cortex. *J Neurosci* 2010; 30: 15298–15303.
10. Jakoby P, Schmidt E, Ruminot I, et al. Higher transport and metabolism of glucose in astrocytes compared with neurons: a multiphoton study of hippocampal and cerebellar tissue slices. *Cereb Cortex* 2012; 24(1): 222–231.
11. Patel AB, Lai JC, Chowdhury GM, et al. Direct evidence for activity-dependent glucose phosphorylation in neurons with implications for the astrocyte-to-neuron lactate shuttle. *Proc Natl Acad Sci U S A* 2014; 111: 5385–5390.
12. Lundgaard I, Li B, Xie L, et al. Direct neuronal glucose uptake heralds activity-dependent increases in cerebral metabolism. *Nat Commun* 2015; 6: 6807.
13. Díaz-García CM, Mongeon R, Lahmann C, et al. Neuronal stimulation triggers neuronal glycolysis and not lactate uptake. *Cell Metab* 2017; 26: 361–374.
14. Bittner CX, Loaiza A, Ruminot I, et al. High resolution measurement of the glycolytic rate. *Front Neuroenerget* 2010; 2: 26.
15. Bittner CX, Valdebenito R, Ruminot I, et al. Fast and reversible stimulation of astrocytic glycolysis by K+ and a delayed and persistent effect of glutamate. *J Neurosci* 2011; 31: 4709–4713.
16. Ruminot I, Gutiérrez R, Peña-Münzenmayer G, et al. NBCe1 mediates the acute stimulation of astrocytic glycolysis by extracellular K+. *J Neurosci* 2011; 31: 14264–14271.
17. Takano T, He W, Han X, et al. Rapid manifestation of reactive astrogliosis in acute hippocampal brain slices. *Glia* 2014; 62: 78–95.
18. Fiala JC, Kirov SA, Feinberg MD, et al. Timing of neuronal and glial ultrastructure disruption during brain slice preparation and recovery in vitro. *J Comp Neurol* 2003; 465: 90–103.
19. Lipton P. Regulation of glycogen in the dentate gyrus of the in vitro guinea pig hippocampus; effect of combined deprivation of glucose and oxygen. *J Neurosci Meth* 1989; 28: 147–154.
20. Galow LV, Schneider J, Lewen A, et al. Energy substrates that fuel fast neuronal network oscillations. *Front Neurosci* 2014; 8: 398.
21. Takanaga H, Chaudhuri B and Frommer WB. GLUT1 and GLUT9 as major contributors to glucose influx in HepG2 cells identified by a high sensitivity intramolecular FRET glucose sensor. *Biochim Biophys Acta* 2008; 1778: 1091–1099.
22. San Martin A, Ceballo S, Baeza-Lehnert F, et al. Imaging mitochondrial flux in single cells with a FRET sensor for pyruvate. *PloS One* 2014; 9: e85780.
23. San Martin A, Ceballo S, Ruminot I, et al. A genetically encoded FRET lactate sensor and its use to detect the Warburg effect in single cancer cells. *PloS One* 2013; 8: e57712.
24. Stoppini L, Buchs P-A and Muller D. A simple method for organotypic cultures of nervous tissue. *J Neurosci Meth* 1991; 37: 173–182.
25. Schneider J, Lewen A, Ta T-T, et al. A reliable model for gamma oscillations in hippocampal tissue. *J Neurosci Res* 2015; 93: 1067–1078.
26. Gawenis LR, Bradford EM, Prasad V, et al. Colonic anion secretory defects and metabolic acidosis in mice lacking the NBC1 cotransporter. *J Biol Chem* 2007; 282: 9042–9052.
27. Hou B-H, Takanaga H, Grossmann G, et al. Optical sensors for monitoring dynamic changes of intracellular metabolite levels in mammalian cells. *Nat Protoc* 2011; 6: 1818–1833.
28. San Martin A, Sotelo-Hitschfeld T, Lerchundi R, et al. Single-cell imaging tools for brain energy metabolism: a review. *Neurophotonics* 2014; 1: 011004.
29. Kann O. The energy demand of fast neuronal network oscillations: insights from brain slice preparations. *Front Pharmacol* 2011; 2: 90.
30. Guy Y, Rupert AE, Sandberg M, et al. A simple method for measuring organotypic tissue slice culture thickness. *J Neurosci Meth* 2011; 199: 78–81.
31. Fishbein WN, Davis JI, Foellmer JW, et al. Clinical assay of the human erythrocyte lactate transporter: II. Analysis and display of normal human data. *Biochem Med Metab Biol* 1988; 39: 351–359.

32. Garcia CK, Goldstein JL, Pathak RK, et al. Molecular characterization of a membrane transporter for lactate, pyruvate, and other monocarboxylates: implications for the Cori cycle. *Cell* 1994; 76: 865–873.
33. Halestrap AP. Monocarboxylic acid transport. *Compr Physiol* 2013; 3: 1611–1643.
34. Mächler P, Wyss MT, Elsayed M, et al. In vivo evidence for a lactate gradient from astrocytes to neurons. *Cell Metab* 2016; 23: 94–102.
35. Valdebenito R, Ruminot I, Garrido-Gerter P, et al. Targeting of astrocytic glucose metabolism by beta-hydroxybutyrate. *J Cereb Blood Flow Metab* 2016; 36: 1813–1822.
36. Liotta A, Rösner J, Huchzermeyer C, et al. Energy demand of synaptic transmission at the hippocampal Schaffer-collateral synapse. *J Cereb Blood Flow Metab Off* 2012; 32: 2076–2083.
37. Kofuji P and Newman E. Potassium buffering in the central nervous system. *Neuroscience* 2004; 129: 1043–1054.
38. Chesler M and Kraig RP. Intracellular pH of astrocytes increases rapidly with cortical stimulation. *Am J Physiol* 1987; 253: R666–R6670.
39. Chesler M and Kraig RP. Intracellular pH transients of mammalian astrocytes. *J Neurosci* 1989; 9: 2011–2019.
40. Deitmer JW and Szatkowski M. Membrane potential dependence of intracellular pH regulation by identified glial cells in the leech central nervous system. *J Physiol* 1990; 421: 617–631.
41. Pappas CA and Ransom BR. Depolarization-induced alkalinization (DIA) in rat hippocampal astrocytes. *J Neurophysiol* 1994; 72: 2816–2826.
42. Gatto C, Arnett KL and Milanick MA. Divalent cation interactions with Na, K-ATPase cytoplasmic cation sites: implications for the para-nitrophenyl phosphatase reaction mechanism. *J Membr Biol* 2007; 216: 49–59.
43. Kofuji P and Newman E. Potassium buffering in the central nervous system. *Neuroscience* 2004; 129: 1043–1054.
44. Kafitz KW, Meier SD, Stephan J, et al. Developmental profile and properties of sulforhodamine 101 – labeled glial cells in acute brain slices of rat hippocampus. *J Neurosci Meth* 2008; 169: 84–92.
45. Theparambil SM, Weber T, Schmalzle J, et al. Proton Fall or Bicarbonate Rise: Glycolytic rate in mouse astrocytes is paved by intracellular alkalinization. *J Biol Chem* 2016; 291: 19108–19117.
46. Trivedi B and Danforth WH. Effect of pH on the kinetics of frog muscle phosphofructokinase. *J Biol Chem* 1966; 241: 4110–4114.
47. Sotelo-Hitschfeld T, Niemeyer MI, Mächler P, et al. Channel-mediated lactate release by K+-stimulated astrocytes. *J Neurosci* 2015; 35: 4168–4178.
48. Karagiannis A, Sylantyev S, Hadjihambi A, et al. Hemichannel-mediated release of lactate. *J Cereb Blood Flow Metab* 2016; 36: 1202–1211.
49. Chesler M. Regulation and modulation of pH in the brain. *Physiol Rev* 2003; 83: 1183–221.
50. Raimondo JV, Tomes H, Irkle A, et al. Tight Coupling of Astrocyte pH Dynamics to Epileptiform Activity Revealed by Genetically Encoded pH Sensors. *J Neurosci* 2016; 36: 7002–7013.
51. Zhang Y, Chen K, Sloan SA, et al. An RNA-sequencing transcriptome and splicing database of glia, neurons, and vascular cells of the cerebral cortex. *J Neurosci* 2014; 34: 11929–11947.
52. Giffard RG, Papadopoulos MC, Van Hooft JA, et al. The electrogenic sodium bicarbonate cotransporter: developmental expression in rat brain and possible role in acid vulnerability. *J Neurosci* 2000; 20: 1001–1008.
53. Schmitt BM, Berger UV, Douglas RM, et al. Na/HCO3 cotransporters in rat brain: expression in glia, neurons, and choroid plexus. *J Neurosci* 2000; 20: 6839–6848.
54. Azarias G, Perreten H, Lengacher S, et al. Glutamate transport decreases mitochondrial pH and modulates oxidative metabolism in astrocytes. *J Neurosci* 2011; 31: 3550–3559.
55. McKhann GM, D'Ambrosio R and Janigro D. Heterogeneity of astrocyte resting membrane potentials and intercellular coupling revealed by whole-cell and gramicidin-perforated patch recordings from cultured neocortical and hippocampal slice astrocytes. *J Neurosci* 1997; 17: 6850–6863.
56. Brookes N and Yarowsky PJ. Determinants of deoxyglucose uptake in cultured astrocytes: the role of the sodium pump. *J Neurochem* 1985; 44: 473–479.
57. Peng L, Zhang X and Hertz L. High extracellular potassium concentrations stimulate oxidative metabolism in a glutamatergic neuronal culture and glycolysis in cultured astrocytes but have no stimulatory effect in a GABAergic neuronal culture. *Brain Res* 1994; 663: 168–172.
58. Peng L, Juurlink BH and Hertz L. Pharmacological and developmental evidence that the potassium-induced stimulation of deoxyglucose uptake in astrocytes is a metabolic manifestation of increased Na(+)-K(+)-ATPase activity. *Dev Neurosci* 1996; 18: 353–359.
59. Abe T, Takahashi S and Suzuki N. Oxidative metabolism in cultured rat astroglia: effects of reducing the glucose concentration in the culture medium and of D-aspartate or potassium stimulation. *J Cereb Blood Flow Metab* 2006; 26: 153–160.
60. Takahashi S, Driscoll BF, Law MJ, et al. Role of sodium and potassium ions in regulation of glucose metabolism in cultured astroglia. *Proc Natl Acad Sci* 1995; 92: 4616–4620.
61. Choi HB, Gordon GRJ, Zhou N, et al. Metabolic communication between astrocytes and neurons via bicarbonate-responsive soluble adenylyl cyclase. *Neuron* 2012; 75: 1094–104.
62. De Simoni A, Griesinger CB and Edwards FA. Development of rat CA1 neurones in acute versus organotypic slices: role of experience in synaptic morphology and activity. *J Physiol* 2003; 550: 135–47.
63. Dyhrfjeld-Johnsen J, Berdichevsky Y, Swiercz W, et al. Interictal spikes precede ictal discharges in an organotypic hippocampal slice culture model of epileptogenesis. *J Clin Neurophysiol* 2010; 27: 418–24.
64. Benediktsson AM, Schachtele SJ, Green SH, et al. Ballistic labeling and dynamic imaging of astrocytes in organotypic hippocampal slice cultures. *J Neurosci Meth* 2005; 141: 41–53.